Electronic Supplementary Information (ESI)

[Pb(Tab)$_2$(4,4'-Bipy)](PF$_6$)$_2$: two-step ambient temperature quantitative solid-state synthesis, structure and dielectric properties

Fan Wang,[a] Chun-Yan Ni,[a] Quan Liu,[a] Fu-Ling Li,[a] Jing Shi,[a] Hong-Xi Li,[a] and Jian-Ping Lang*[a,b]

[a] College of Chemistry, Chemical Engineering and Materials Science, Soochow University, Suzhou 215123, Jiangsu, P. R. China.

[b] State Key Laboratory of Organometallic Chemistry, Shanghai Institute of Organic Chemistry, Chinese Academy of Sciences, Shanghai 200032, P. R. China

Table of Contents

Experimental Section······S3

General

Synthesis of **1** and **2**

X-ray Crystallographic Study

Table S1. Summary of crystallographic data for **1**·2MeCN·DMF and **2**·2MeCN.······S6

Table S2. Selected bond lengths (Å) and angles (°) for **1** and **2**.······S7

Fig. S1. (a) Ambient temperature solid-state reaction of $Pb(OAc)_2$ with $TabHPF_6$ afforded $[Pb(Tab)_2]_2(PF_6)_4$. (b) Ambient temperature solid-state reaction of **1** with 4,4'-bipy generated $[Pb(Tab)_2(4,4'\text{-bipy})](PF_6)_2$.······S8

Fig. S2. (a) The Raman spectra of **1** and **1**·2MeCN·DMF. (b) The Raman spectra of **2** and **2**·2MeCN.······S9

Fig. S3. (a) The TGA curves for **1**. (b) The TGA curves for **2**.······S9

Fig. S4. (a) The XPS Pb4f core level spectra for **1** (blue line) and **1**·2MeCN·DMF (red line). (b) The XPS Pb4f core level spectra for **2** (blue line) and **2**·2MeCN (red line).······S9

Fig. S5. The PXRD patterns of two compounds (black: powder; blue: crystal without solvents; green: crystal with solvents; red: simulated). (a) The patterns of **1**. (b) The patterns of **2**.······S10

Fig. S6. (a) The solid state emission spectra of **1** (blue line) and **1**·2MeCN·DMF (red line) (excitation at 406 nm). (b) The solid state emission spectra of **2** (blue line) and **2**·2MeCN (red line) (excitation at 406 nm).······S10

Fig. S7. Temperature dependence of the dielectric permittivity (ε) or dielectric loss (*DL*) at different frequency. (a) ε of **1**. (b) *DL* of **1**. (c) ε of **2**. (d) *DL* of **2**. (e) ε of $Pb(OAc)_2$. (f) *DL* of $Pb(OAc)_2$.······S11

Fig. S8. Frequency dependence of the dielectric permittivity (ε) and dielectric loss (*DL*) of two compounds and $Pb(OAc)_2$ at 30 °C. (a) The ε of **1**, **2** and $Pb(OAc)_2$. (b) The *DL* of **1**, **2** and $Pb(OAc)_2$.······S12

Experimental Section

General. $TabHPF_6$ was prepared according to the literature procedures previously reported.[1] Solvents like DMF and MeCN were dried over CaH_2 and distilled in vacuo. All chemicals and reagents were obtained from commercial sources and used as received. The elemental analyses for C, H, N were performed on a Carlo-Erba CHNO-S microanalyzer. The IR spectra were recorded on a Varian 1000 FT-IR spectrometer as KBr disks (4000-400 cm^{-1}). ^1H NMR spectra were recorded at ambient temperature on a Varian UNITY plus–400 spectrometer. The ^1H NMR chemical shifts were referenced to TMS in $CDCl_3$. The powder X-ray diffraction (PXRD) measurements were carried out on a PANalytical X'Pert PRO MPD system (PW3040/60). The Raman spectra were recorded on a LabRam I confocal micro-Raman system from Dilor (HR800). XPS measurements were carried out on a Perkin-Elmer PHI 550 ESCA/SAM photoelectron spectrometer using Al Kα line (1486.6eV) radiation taking carbon $1S_{1/2}$ binding energy (285.0eV) as a standard. Thermal analysis was performed with a Perkin-Elmer TGA–7 thermogravimetric analyser at a heating rate of 10 °C/min in air. The photoluminescent spectra were obtained on a Perkin-Elmer LS55 spectrofluorometer.

Synthesis of 1. White powders of $Pb(OAc)_2$ (0.2 mmol, 59 mg) and $TabHPF_6$ (0.4 mmol, 125 mg) were mixed and ground in an agate mortar at room temperature. The color of the mixture was turned light yellow gradually with the obvious smell of acetic acid coming out. After grinding the mixture for 30 min and slightly irradiating the resulting product using an IR lamp to remove the acetic acid, it formed a yellow solid $[Pb(Tab)_2]_2(PF_6)_4$ (**1**). Yield: 166 mg, (100%). Anal. Calcd. for $C_{36}H_{52}F_{24}N_4P_4Pb_2S_4$: C, 25.99; H, 3.16; N, 3.37. Found: C, 26.28; H, 3.18; N, 3.38. IR (KBr disk): 1644 (s), 1582 (w), 1489 (s), 1124 (m), 1010 (m), 958 (m), 838 (s), 746 (m), 558 (s) cm^{-1}. ^1H NMR (400 MHz, $CDCl_3$): δ 3.824 (s, 9H, -Me), 7.550-7.868 (m, 4H, -Ph). Light yellow plate crystals of **1**·2MeCN·DMF were obtained from dissolving **1** (166 mg) in mixed MeCN and DMF (v/v = 1 : 1) followed by layering the solution with Et_2O several days later. Yield: 148 mg (89%). Anal. Calcd. for $C_{43}H_{65}F_{24}N_7OP_4Pb_2S_4$: C, 28.40; H, 3.61; N, 5.39. Found: C, 28.47; H, 3.56; N, 5.38. IR (KBr disk): 1645 (s), 1580 (w), 1487 (s), 1125 (m), 1011 (m), 956 (m), 837 (s), 744 (m), 559 (s) cm^{-1}. The solvent molecules of **1**·2MeCN·DMF can be readily removed *in vacuo*. Anal. Calcd. for $C_{36}H_{52}F_{24}N_4P_4Pb_2S_4$: C, 25.99; H, 3.15; N, 3.37. Found: C, 25.87; H, 3.13; N, 3.40. IR (KBr disk): 1644 (s), 1581 (w), 1490 (s), 1125 (m), 1012 (m), 959 (m), 837 (s), 746 (m), 557 (s) cm^{-1}.

Synthesis of 2. A solid mixture containing complex **1** (0.1 mmol, 166 mg) and 4,4'-bipy (0.2 mmol, 31 mg) was well ground at ambient temperature for 30 min. It afforded another yellow solid [Pb(Tab)$_2$(4,4'-bipy)](PF$_6$)$_2$ (**2**). Yield: 197 mg (100%). Anal. Calcd. for $C_{28}H_{34}F_{12}N_4P_2PbS_2$: C, 34.04; H, 3.47; N, 5.67. Found: C, 33.88; H, 3.45; N, 5.62. IR (KBr disk): 1598 (m), 1488 (s), 1384 (m), 1124 (m), 1010 (m), 837 (s), 744 (m), 557 (s) cm^{-1}. ^{1}H NMR (400 MHz, CDCl$_3$): δ 3.796 (s, 9H, -Me), 7.535-7.827 (m, 4H, -Ph), 7.837-8.020 (m, 4H, -4,4'-bipy). The yellow prismatic crystals of **2**·2MeCN were obtained by dissolving **1** (197 mg) in MeCN followed by layering the solution with Et$_2$O several days later. Yield: 170 mg (86%). Anal. Calcd. for $C_{32}H_{40}F_{12}N_6P_2PbS_2$: C, 35.92; H, 3.77; N, 7.85. Found: C, 35.86; H, 3.74; N, 7.88. IR (KBr disk): 1599 (m), 1488 (s), 1383 (m), 1125 (m), 1011 (m), 836 (s), 745 (m), 559 (s) cm^{-1}. The solvent molecules of **2**·2MeCN can be easily removed *in vacuo*. Anal. Calcd. for $C_{28}H_{34}F_{12}N_4P_2PbS_2$: C, 34.04; H, 3.47; N, 5.67. Found: C, 34.18; H, 3.53; N, 5.71. IR (KBr disk): 1598 (m), 1487 (s), 1385 (m), 1125 (m), 1011 (m), 837 (s), 744 (m), 558 (s) cm^{-1}.

X-ray Crystallographic Study. Diffraction intensities of **1**·2MeCN·DMF and **2**·2MeCN were collected on a Rigaku Mercury CCD X-ray diffractometer (Mo Kα, λ = 0.71073 Å). The single crystals of **1**·2MeCN·DMF and **2**·2MeCN were mounted at the top of a glass fiber with grease at 223 K in a stream of gaseous nitrogen. Cell parameters were refined on all observed reflections by using the program *CrystalClear* (Rigaku and MSc, Ver. 1.3, 2001). The collected data were reduced by the program *CrystalClear*, and an absorption correction (multi-scan) was applied. The reflection data were also corrected for Lorentz and polarization effects.

The crystal structures of **1**·2MeCN·DMF and **2**·2MeCN were solved by direct methods[2] and refined on F^2 by full-matrix least-squares techniques with *SHELXTL-97* program. For **2**·2MeCN, one MeCN solvated molecule was disordered over two positions with an occupancy ratio of C31-C32-N6/C31A-C32A-N6A = 0.48/0.52. The F atoms of PF_6^- anions were disordered over two sits with an occupancy factor of P1~P6/P1A~P6A = 0.61/0.39 and P7~P12/P7A~P12A = 0.68/0.32. The methyl groups of one Tab ligand were disordered over two sites with an occupancy ratio of C17-C18-C19/ C17A-C18A-C19A = 0.77/0.23. All non-hydrogen atoms, except for one MeCN solvent molecule in **2**·2MeCN were refined anisotropically. Hydrogen atoms were placed in geometrically idealized positions and constrained to ride on their parent atoms. All the calculations were performed on a Dell workstation using the *CrystalStructure* crystallographic software package (Rigaku and MSC, Ver.3.60, 2004).

References

1. B. V. DePamphilis, B. A. Averill, T. Herskovitz, L. Que, Jr., R. H. Holm, *J. Am. Chem. Soc*. 1974, **96**, 4159.

2. (a) G. M. Sheldrick, *SHELXS-97, Program for Solution of Crystal Structures*; University of Göttingen: Göttingen, Germany, 1997. (b) G. M. Sheldrick, *SHELXL-97, Program for Refinement of Crystal Structures*; University of Göttingen, Göttingen, Germany, 1997.

Table S1. Summary of crystallographic data for **1**·2MeCN·DMF and **2**·2MeCN.

Compound	**1**·2MeCN·DMF	**2**·2MeCN
Empirical Formula	$C_{43}H_{65}F_{24}N_7OP_4Pb_2S_4$	$C_{32}H_{40}F_{12}N_6P_2PbS_2$
Formula Weight	1818.52	1069.95
Crystal System	monoclinic	monoclinic
Space Group	*C*2	*C*2/*c*
a (Å)	37.896(6)	41.814(8)
b (Å)	12.929(2)	8.9420(2)
c (Å)	12.973(2)	22.936(5)
β (°)	95.194(1)	105.692(4)
V (Å^3)	6330.3(2)	8256(3)
Z	4	8
ρ_{calc} (g/cm^3)	1.908	1.722
F(000)	3536	4208
μ (MoKα,mm^{-1})	5.656	4.352
Total reflections	26276	43828
Unique reflection	11005 (R_{int} = 0.0847)	9366 (R_{int} = 0.0551)
No. observations	10436 ($I > 2.00\sigma(I)$)	8847 ($I > 2.00\sigma(I)$)
No. parameters	506	623
R^a	0.0962	0.0462
$R_w{}^b$	0.2331	0.0985
GOF^c	1.068	1.174

[a] $R = \Sigma||F_o|-|F_c||/\Sigma|F_o|$. [b] $R_w = \{\Sigma w(F_o{}^2-F_c{}^2)^2/\Sigma w(F_o{}^2)^2\}^{1/2}$. [c] GOF = $\{\Sigma w((F_o{}^2-F_c{}^2)^2)/(n-p)\}^{1/2}$, where M is the number of reflections and N is the number of parameters.

Table S2. Selected bond lengths (Å) and angles (°) for **1** and **2**.

Compound **1**

Pb(1)-S(1)	2.688(5)	Pb(1)-S(1)#1	2.688(5)	Pb(1)-S(2)#1	3.013(6)
Pb(1)-S(2)	3.013(6)	Pb(2)-S(4)	2.650(6)	Pb(2)-S(2)	2.763(6)
Pb(2)-S(3)	2.852(6)	Pb(2)-S(1)#1	3.061(5)	Pb(2)-Pb(3)	3.6881(18)
Pb(3)-Pb(3)#2	2.150(3)	Pb(3)-S(3)#2	2.774(6)	Pb(3)-S(3)	2.816(6)
Pb(3)-S(4)	2.846(6)	S(1)-C(1)	1.77(2)	S(1)-Pb(2)#1	3.061(5)
S(2)-C(10)	1.738(19)	S(3)-C(19)	1.76(2)	S(3)-Pb(3)#2	2.774(6)
S(4)-C(28)	1.77(2)				
S(1)-Pb(1)-S(1)#1	83.0(2)	S(1)-Pb(1)-S(2)#1	80.46(15)	S(1)#1-Pb(1)-S(2)#1	87.02(16)
S(1)-Pb(1)-S(2)	87.02(16)	S(1)#1-Pb(1)-S(2)	80.46(15)	S(2)#1-Pb(1)-S(2)	163.3(2)
S(4)-Pb(2)-S(2)	87.05(19)	S(4)-Pb(2)-S(3)	79.57(15)	S(2)-Pb(2)-S(3)	80.76(17)
S(4)-Pb(2)-S(1)#1	85.70(15)	S(2)-Pb(2)-S(1)#1	78.47(14)	S(3)-Pb(2)-S(1)#1	155.06(16)
S(4)-Pb(2)-Pb(3)	50.16(13)	S(2)-Pb(2)-Pb(3)	114.32(14)	S(3)-Pb(2)-Pb(3)	48.99(12)
S(1)#1-Pb(2)-Pb(3)	130.61(10)	Pb(3)#2-Pb(3)-S(3)#2	68.43(13)	Pb(3)#2-Pb(3)-S(3)	66.35(12)
S(3)#2-Pb(3)-S(3)	84.3(2)	Pb(3)#2-Pb(3)-S(4)	133.74(11)	S(3)#2-Pb(3)-S(4)	81.19(17)
S(3)-Pb(3)-S(4)	76.99(16)	Pb(3)#2-Pb(3)-Pb(2)	115.04(8)	S(3)#2-Pb(3)-Pb(2)	111.32(13)
S(3)-Pb(3)-Pb(2)	49.84(11)	S(4)-Pb(3)-Pb(2)	45.64(11)	C(1)-S(1)-Pb(1)	101.0(7)
C(1)-S(1)-Pb(2)#1	115.3(6)	Pb(1)-S(1)-Pb(2)#1	90.89(14)	C(10)-S(2)-Pb(2)	106.5(7)
C(10)-S(2)-Pb(1)	106.0(7)	Pb(2)-S(2)-Pb(1)	90.46(18)	C(19)-S(3)-Pb(3)#2	87.9(7)
C(19)-S(3)-Pb(3)	109.6(7)	Pb(3)#2-S(3)-Pb(3)	45.22(11)	C(19)-S(3)-Pb(2)	103.2(7)
Pb(3)#2-S(3)-Pb(2)	125.1(2)	Pb(3)-S(3)-Pb(2)	81.17(16)	C(28)-S(4)-Pb(2)	110.0(7)

C(28)-S(4)-Pb(3)	100.4(7)	Pb(2)-S(4)-Pb(3)	84.20(16)

Compound **2**

Pb(1)-N(1)	2.49 (4)	Pb(1)-S(1)	2.715(12)	Pb(1)-S(2)	2.762(12)
P(2)-F(10A)	1.4(2)	P(2)-F(12A)	1.5(2)	P(2)-F(8A)	1.53(16)
P(2)-F(7A)	1.53(19)	P(2)-F(9)	1.55(11)	P(2)-F(11A)	1.6(2)
P(2)-F(11)	1.56(12)	P(2)-F(7)	1.57(10)	P(2)-F(8)	1.57(9)
P(2)-F(9A)	1.6(2)	P(2)-F(12)	1.58(9)	P(2)-F(10)	1.63(10)
S(1)-C(11)	1.76(5)	S(2)-C(20)	1.76(5)		
N(1)-Pb(1)-S(1)	81.9(10)	N(1)-Pb(1)-S(2)	83.0(10)	S(1)-Pb(1)-S(2)	86.8(4)

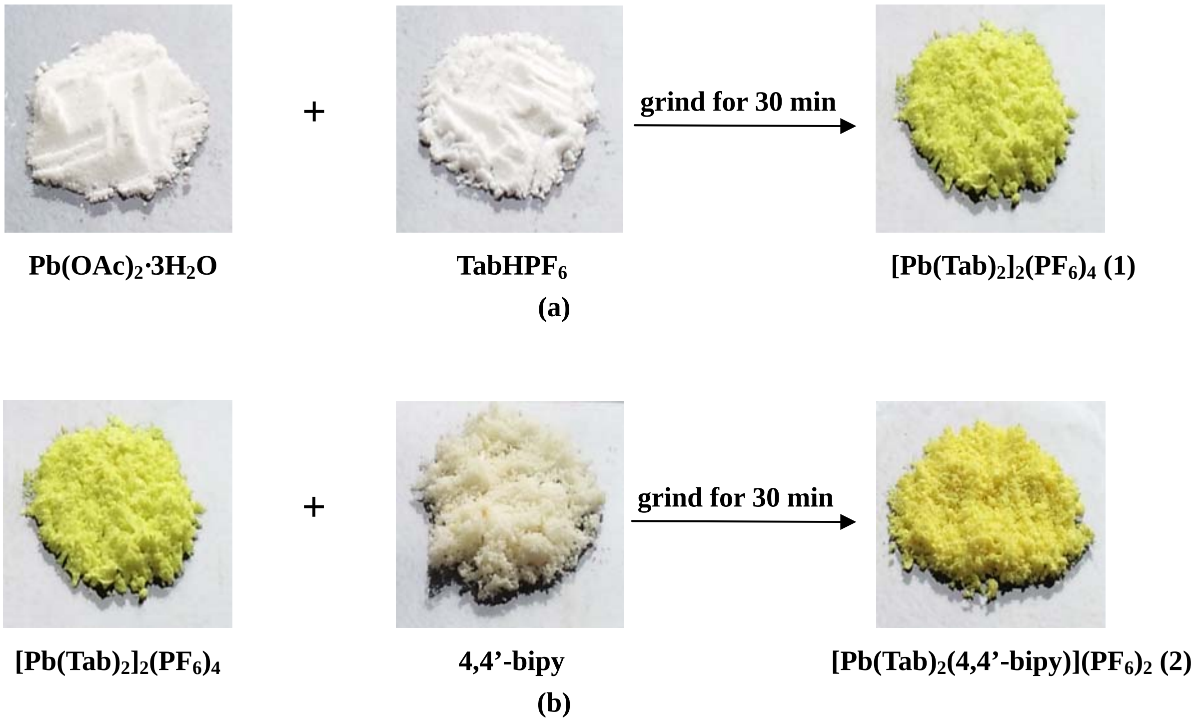

Fig. S1. (a) Ambient temperature solid-state reaction of $Pb(OAc)_2$ with $TabHPF_6$ afforded $[Pb(Tab)_2]_2(PF_6)_4$. (b) Ambient temperature solid-state reaction of **1** with 4,4'-bipy generated $[Pb(Tab)_2(4,4'\text{-bipy})](PF_6)_2$.

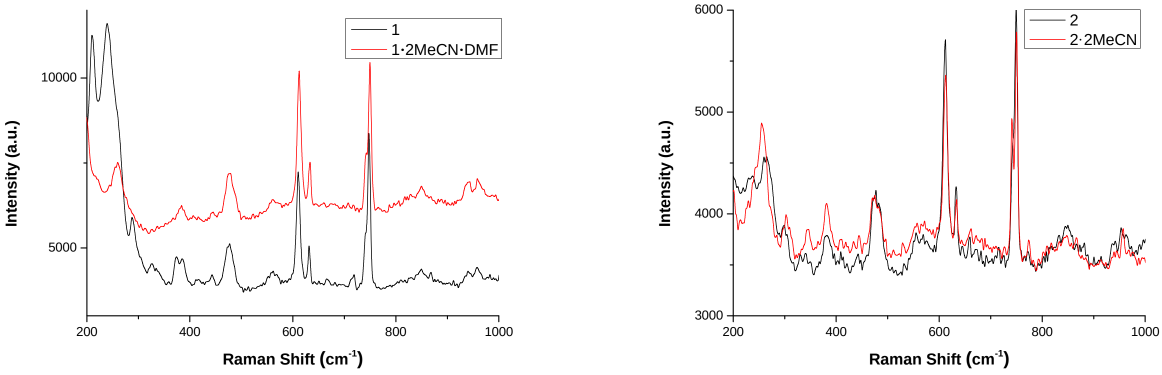

(a) **(b)**

Fig. S2. (a) The Raman spectra of **1** and **1**·2MeCN·DMF. (b) The Raman spectra of **2** and **2**·2MeCN.

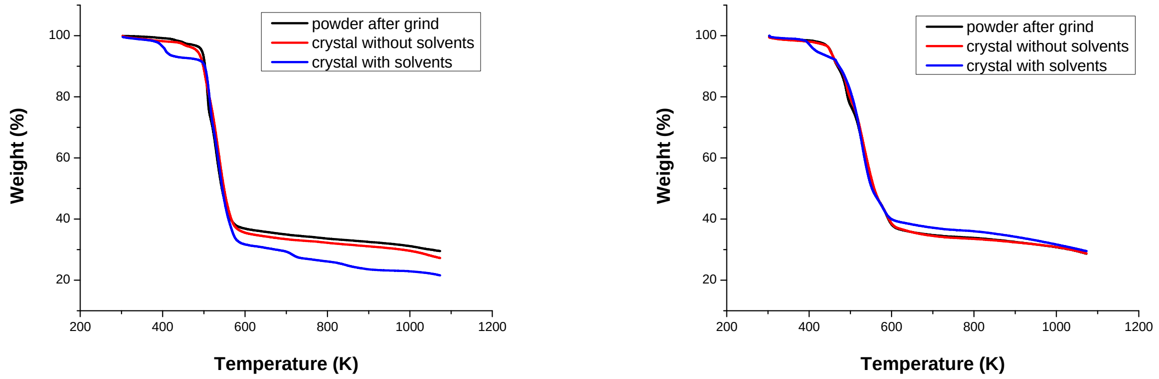

(a) **(b)**

Fig. S3. (a) The TGA curves for **1**. (b) The TGA curves for **2**.

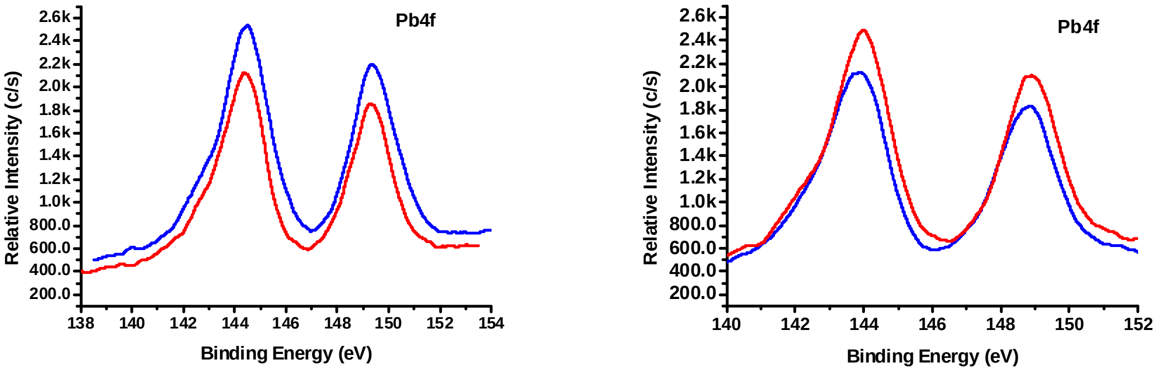

(a) **(b)**

Fig. S4. (a) The XPS Pb4f core level spectra for **1** (blue line) and **1**·2MeCN·DMF (red line). (b) The XPS Pb4f core level spectra for **2** (blue line) and **2**·2MeCN (red line).

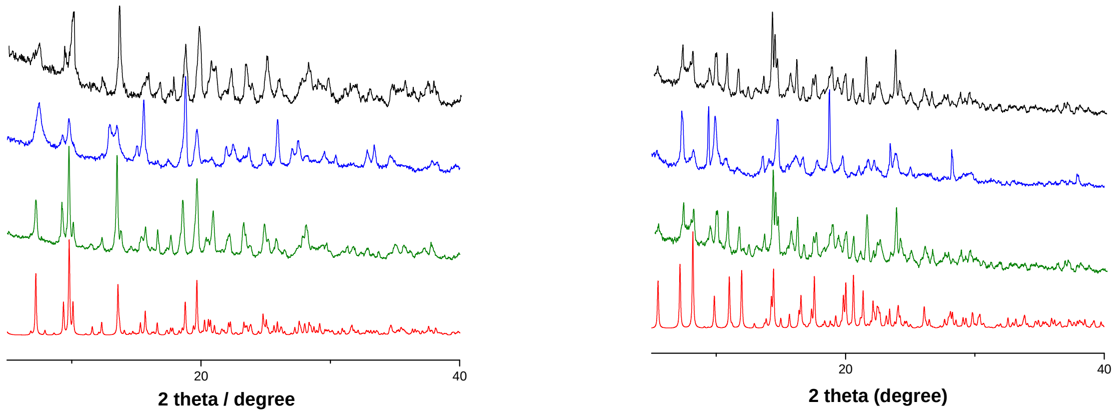

(a)

(b)

Fig. S5. The PXRD patterns of two compounds (black: powder; blue: crystal without solvents; green: crystal with solvents; red: simulated). (a) The patterns of **1**. (b) The patterns of **2**.

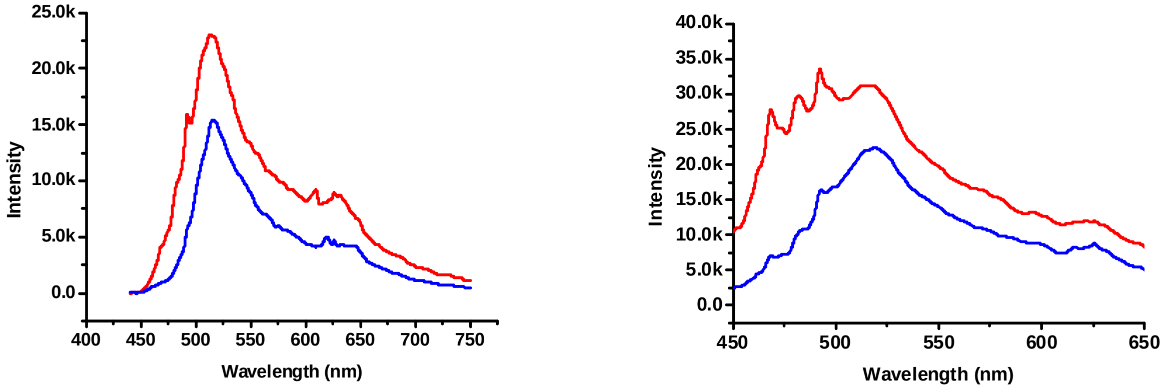

(a)

(b)

Fig. S6. (a) The solid state emission spectra of **1** (blue line) and **1**·2MeCN·DMF (red line) (excitation at 406 nm). (b) The solid state emission spectra of **2** (blue line) and **2**·2MeCN (red line) (excitation at 406 nm).

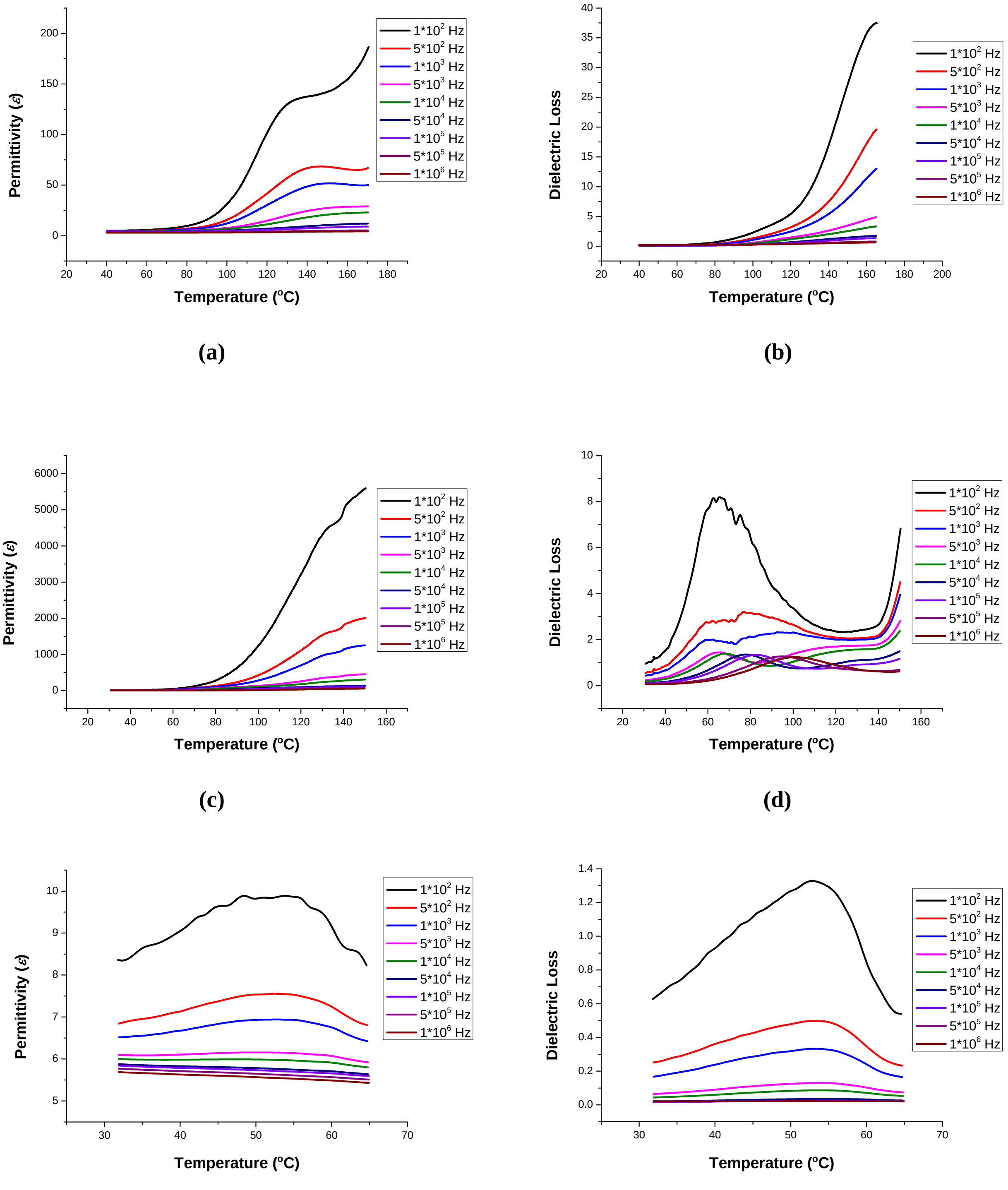

(a) **(b)**

(c) **(d)**

(e) **(f)**

Fig. S7. Temperature dependence of the dielectric permittivity (*ε*) or dielectric loss (*DL*) at different frequency. (a) *ε* of **1**. (b) *DL* of **1**. (c) *ε* of **2**. (d) *DL* of **2**. (e) *ε* of Pb(OAc)$_2$. (f) *DL* of Pb(OAc)$_2$.

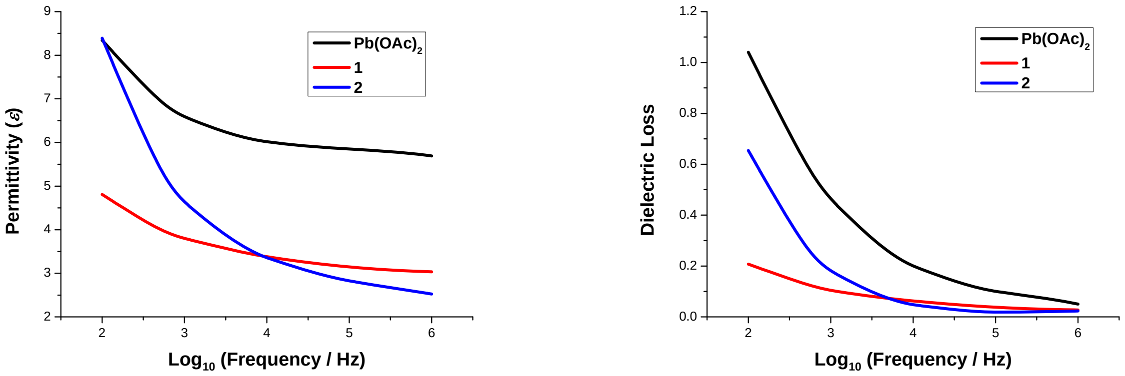

(a) **(b)**

Fig. S8. Frequency dependence of the dielectric permittivity (*ε*) and dielectric loss (*DL*) of two compounds and $Pb(OAc)_2$ at 30 ºC. (a) The *ε* of **1**, **2** and $Pb(OAc)_2$. (b) The *DL* of **1**, **2** and $Pb(OAc)_2$.